

MICROSTRUCTURE CHARACTERISTICS OF Cr₃C₂-NiCr COATINGS DEPOSITED WITH THE HIGH-VELOCITY OXY-FUEL THERMAL-SPRAY TECHNIQUE

KARAKTERISTIKE MIKROSTRUKTUR Cr₃C₂-NiCr PREVLEK IZDELANIH S TEHNIKO NAPRŠEVANJA V TOKU PLINSKE MEŠANICE KISIKA IN PROPANA Z VELIKO HITROSTJO

Jason Lauzuardy^{1,2}, Eddy Agus Basuki¹, Erie Martides², Selly Septianissa³,
Budi Prawara², Dedi⁴, Endro Junianto⁵, Edy Riyanto^{2,*}

¹Department of Metallurgical Engineering, Faculty of Mining and Petroleum Engineering, Institut Teknologi Bandung, Bandung 40132, Indonesia

²Research Center for Advanced Materials, National Research and Innovation Agency, Serpong 15314, Indonesia

³Department of Mechanical Engineering, Faculty of Engineering, Widyatama University, Bandung 40125, Indonesia

⁴Research Center for Electronics, National Research and Innovation Agency, Bandung 40135, Indonesia

⁵Research Center for Smart Mechatronics, National Research and Innovation Agency, Bandung 40135, Indonesia

Prejem rokopisa – received: 2023-05-03; sprejem za objavo – accepted for publication: 2024-01-22

doi:10.17222/mit.2023.869

With the goals of protecting boiler tubes from hostile surroundings, increasing thermal efficiency, and minimizing time losses from damage, thermal-spray coating methods for high-temperature operations were created. Ceramic-metal composite materials (e.g., Cr₃C₂-NiCr) are well known for protecting components from erosion decay in a high-temperature environment. In this investigation, the high-velocity oxy-fuel (HVOF) thermal-spray technique was employed to successfully deposit several variations of feedstocks containing Cr₃C₂-NiCr and NiCr powders onto a medium-carbon steel substrate, with and without filtering through a 400-mesh screen. Utilizing X-ray fluorescence (XRF), scanning electron microscopy (SEM), energy dispersive spectroscopy (EDS) and X-ray diffraction (XRD), the microstructure features of the deposited coatings were assessed. The experiment results demonstrate that the crystallite and grain sizes of the deposited coatings can be increased by reducing the powder size through a sifting process using a 400-mesh sieve. This procedure also resulted in a coating with a higher density and lower porosity. Furthermore, new compounds including Cr₂O₃ and MnCr₂O₄ were formed in the coating layers as indicated by the XRD spectra. These phenomena are in good agreement with the EDS mapping of Cr and O, which reveals highly similar distributions. Manganese was originally a part of the substrate composition. Manganese could diffuse rapidly across the Cr₂O₃ layer and form the MnCr₂O₄ compound, indicating the manganese diffusion from the substrate into the Cr₃C₂-NiCr coating. The formation of MnCr₂O₄ can be attributed to the prior emergence of the Cr₂O₃ compound.

Keywords: thermal-spray coating, high-velocity oxy-fuel coating, ceramic-metal material, Cr₃C₂-NiCr coating

Z namenom, da bi se cevi boilerjev zaščitile pred škodljivimi vplivi okolice, povečala njihova toplotna učinkovitost in zmanjšale časovne izgube zaradi poškodb oziroma vzdrževanja, se v novejšem času za nanašanje tankih zaščitnih slojev uporabljajo metode termičnega naprševanja v toku plinske mešanice kisika in propana z veliko hitrostjo (HVOF; angl.: high velocity oxy-fuel thermal spray coating). Za ta namen so danes poznani kot najučinkovitejši kompozitni materiali keramika-kovina (to je: Cr₃C₂-NiCr), ki uspešno preprečujejo propadanje komponent (cevi) zaradi visoko temperaturne korozije. V tem članku avtorji opisujejo uporabo termičnega naprševanja zaščitnih plasti s HVOF postopkom. Uspešno so izdelali več vrst zaščitnih plasti (slojev), ki so jih izdelali z omenjenim postopkom. Na podlagi iz srednje ogljičnega jekla so nanašali Cr₃C₂-NiCr in NiCr nefiltrirane prahove ter predhodno presejane prahove na filtru z velikostjo odprtin cca 37 mikrometrov (400 mesh). Za karakterizacijo mikrostrukture izdelanih zaščitnih slojev so uporabili rentgensko fluorescenco (XRF), vrstično elektronsko mikroskopijo (SEM), spektroskopijo na osnovi energije sipanja elektronov (EDS), in rentgensko difrakcijo (XRD). Eksperimentalni rezultati so pokazali, da narašča velikost dendritov in kristalnih zrn z zmanjšanjem količine doziranja prašne mešanice skozi 37 mikrometersko sito. Ta postopek je zmanjšal poroznost in povišal gostoto izdelanih zaščitnih slojev. V XRD spektru so avtorji zaznali tudi nastanek novih spojin, kot sta Cr₂O₃ in MnCr₂O₄. To se je dobro ujemale tudi z izdelano vzdolžno in prečno EDS porazdelitvijo vsebnosti kroma (Cr) in kisika (O). Mangan (Mn) originalno izvira oziroma je difundiral v napršene plasti iz jeklene podlage preko Cr₂O₃ in tvoril MnCr₂O₄. To nakazuje, da se je med naprševanjem Cr₃C₂-NiCr prahu pri visoki temperatur najprej tvoril Cr₂O₃, nato pa je zaradi difuzije Mn iz jeklene podlage v plasteh začela nastajati še faza MnCr₂O₄.

Ključne besede: prevleke izdelane s postopkom termičnega naprševanja z veliko hitrostjo, plinska mešanica kisik (zrak)-propan, keramika-kovina, prevleka na osnovi mešanice prahov Cr₃C₂ in NiCr

1 INTRODUCTION

Surface erosion is a common problem for components that are exposed to environments with sand parti-

cles, such as those used in slurry pumps, boiler tubes, hydro turbines, and pulp handling components.^{1,2} WC-Co, NiCr, WC-CoCr and other cermet-based materials with excellent corrosion resistance and high wear resistance are used for high-velocity oxygen-fuel (HVOF) spraying in a variety of technical applications.^{3,4} To strengthen the resistance to wear caused by abrasion and

*Corresponding author's e-mail:
edy.riyanto@brin.go.id (Edy Riyanto)

Table 1: Chemical composition of the substrate material

Chemical composition	Content, w/%				
	Fe	Mn	Cr	S	Si
ASTM SA210 Grade C	98.90	0.74	0.034	0.057	0.27
Standard ¹⁹	Allowance	0.29–1.06	≤0.35	≤0.035	≥0.10

lengthen the product life and efficiency of steels, particularly in hostile situations with high temperatures, thermal-spray coating has become a vital technique.^{5,6} In boiler applications, for example, wear and corrosion occur at high temperatures, one of the most difficult conditions.⁷ Because there are so many different coating applications, it is necessary to adapt coating qualities to ensure that the substrate and coating work at their best in each particular environment.⁷

Thermal spraying, which creates and projects droplets of molten or semi-molten material onto a substrate to form a coating, is widely used in industries to alleviate the effects of erosion oxidation. Hard-metal coatings (e.g., Cr₃C₂-25NiCr, Cr₃C₂-37WC-18NiCoCr, WC-10Co4Cr) are often applied using high-velocity flame spray methods such as high-velocity oxygen-fuel or high-velocity air-fuel (HVOF) spray procedures.^{7,8} To produce combustion with a fuel, the HVOF spray method uses pure oxygen as the oxidizer, whereas the HVAF spray process uses compressed air.⁷ In general, the HVAF spray process achieves faster particle velocities than the HVOF spray process; however, particle temperatures are lower due to a decreased oxygen content, resulting in a lower combustion temperature.^{1,7} For this reason, the HVAF spray process is a viable alternative to HVOF, while the application equipment and component type define the best spray technique.

For the creation of carbide-based cermet coatings, high-velocity oxygen-fuel technology has gained widespread use.^{9,10} Due to its ability to generate coatings with strong adhesion (bond strength > 70 MPa), low porosity (< 1 %), and low oxide content (< 1 %), the HVOF thermal spraying is one of the best substitutes for chromium.^{11,12} High kinetic energy powder particles acquired during an HVOF process ensure strong coating cohesiveness and enable the production of carbide-based coatings with little decarburization and porosity.¹¹ The HVOF thermal-spray coating method facilitates the production of a very dense layer with low porosity and low residual stress.^{13,14} The process can be used to achieve a high-hardness coating that is very dense and has a high cohesive strength.^{10,15,16} Furthermore, it was found that the coating obtained with 60CrC-40NiCr powder is denser and more homogeneous than that obtained with 75CrC-25NiCr powder as the microhardness of 75CrC-25NiCr is greater than that of 60CrC-40NiCr.¹⁷ On the other hand, new phases can emerge in the coatings obtained with HVOF thermal spraying due to the chemical reaction among the constituents.¹⁸ It was shown that the manganese element that originates from the substrate can diffuse across the HVOF Cr₃C₂-NiCr layer.

Furthermore, this diffusion occurs due to the prior formation of a chromium oxide compound in a Cr₃C₂-NiCr HVOF coating as manganese is able to diffuse rapidly across Cr₂O₃ and develops an MnCr₂O₄ compound over the surface.

2 EXPERIMENTAL PART

Medium-carbon Fe-based boiler steel (ASTM SA210 grade C), commonly used for boiler tubes, was employed as the substrate material. The composition of the steel used as the substrate, which was observed using X-ray fluorescence (XRF), is shown in **Table 1**. The chemical configuration is generally matching the ASME SA210/SA210m standard for medium-carbon steel tubes for boilers and superheaters.¹⁹ A boiler tube was cut in the form of a coupon with dimensions of ≈40 × 30 × 8 mm (**Figure 1d**), which was grit blasted using aluminum oxide (Al₂O₃) with a particle size of 24 mesh before the HVOF spraying process.

Figure 1 shows the substrate preparation from the boiler-tube raw material (ASTM SA210 grade C). The initial raw material is represented in **Figure 1a** as a tube, which was subsequently cut into three portions (**Figure 1b**) to create the substrate (**Figures 1c** and **1d**). To en-

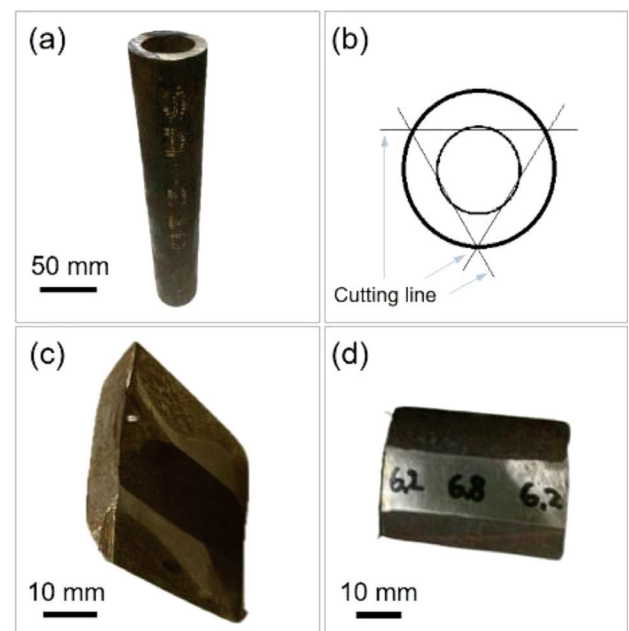


Figure 1: Raw materials and substrate: (a) boiler-tube raw substrate material with ASTM SA210 grade C specifications; (b) a diagram of the boiler tube being sliced to produce the substrate; (c) the substrate's inner side; (d) partially flattened surface of the outer pipe, which serves as the coated substrate

able the coating performance measurement, the curved surface of the substrate was flattened prior to the deposition process as illustrated in **Figure 1d**.

The powders used in this study were Cr₃C₂-NiCr (PAC 131) and NiCr (43C-NS). The deposited powders included 5 powder variations as shown in **Table 2**. A powder was sifted using a 400-mesh sieve agitated by a sieve shaker (450 watt, 50 Hz). The amount of each powder variation was 500 grams. For the mixing process, blending was carried out using a V-type blending machine for 8 hours with a rotational speed of 64 rpm and an ambient temperature of ~28 °C.

Table 2: Variations of the coating powder

Coating powder	Type	Weight (grams)
Cr ₃ C ₂ -NiCr	Original	500
60 % Cr ₃ C ₂ -NiCr + 40 % NiCr	Original	300 + 200
80 % Cr ₃ C ₂ -NiCr + 20 % NiCr	Original	400 + 100
60 % Cr ₃ C ₂ -NiCr + 40 % NiCr	400 mesh	300 + 200
80 % Cr ₃ C ₂ -NiCr + 20 % NiCr	400 mesh	400 + 100

The TECKNOTHERM Hipojet-2700 HVOF was used to perform HVOF spraying at the Coating Laboratory of the National Research and Innovation Agency of the Republic of Indonesia. **Table 3** provides an illustration of the process parameters.

Table 3: HVOF parameters

Parameter		Unit	Value
Air pressure		bar	6.2
Pressure	O ₂	bar	8
	N ₂	bar	5
	Propane	bar	5.5
Flow rate	O ₂	L/min	271
	N ₂	L/min	8
	Propane	L/min	62.4
Powder feeder rotation		min ⁻¹	5
Stand-off distance		mm	200
Spray angle		°	90
Substrate preheating		°C	≤150

Images of the powder, cross-section of the coating and surface view of the coated Cr₃C₂-NiCr were taken with a high-resolution scanning electron microscope (JSM-IT300, JEOL-Japan). This instrument was also employed to detect the chemical composition of the powders and HVOF coatings through energy dispersive spectroscopy (EDS). The formed compounds of the coating were detected using X-ray diffraction (D8 Advance Eco, Bruker, Bragg-Bentano Diffraction). Furthermore, XRD data were also used to measure the crystallite size of the deposited coatings using the Debye-Scherer method. In addition, the pore formation levels were evaluated from SEM images using ImageJ software.

3 RESULTS AND DISCUSSION

Figure 2 shows SEM-EDS micrographs of coating-powder variations. **Figure 2a** shows Cr₃C₂-NiCr, **2c** shows 60 w/% Cr₃C₂-NiCr + 40 w/% NiCr, **2e** shows 80 w/% Cr₃C₂-NiCr + 20 w/% NiCr. In addition, EDS mapping of these powders can be seen in **Figures 2b, 2d** and **2f**, respectively. Characterisation of the coating powders is one of important tasks before they can be applied onto the substrate with the thermal spray method.²⁰ It clearly reveals that the shape of nickel is spherical (**Figures 2b, 2d** and **2f**). Chromium and carbide have an irregular shape (**Figures 2b, 2d** and **2f**). The Cr₃C₂-NiCr powder is the only one that originates from the powder maker (**Figure 2a**). It is shown that there is no visible oxidation element (oxygen) in the EDS mapping of the powder (**Figure 2b**). Meanwhile, the powders that underwent the mixing process have identical chemical contents of Cr, C, Ni and O (**Figures 2d** and **2f**). The presence of O indicates the existence of oxidation that occurred during the mixing process.

Figure 3 shows the surfaces of HVOF coatings (**Figures 3a, 3c, 3e, 3g** and **3i**) and the surface elemental contents measured using EDS (**Figures 3b, 3d, 3f, 3h** and **3j**). It is shown that the surfaces are rough. The microstructures consist of oxide particles, pores, splats, partially melted particles, and unmelted particles (**Figures 3a, 3c, 3e** and **3g**). There are also splats with cracks as shown in **Figures 3a** and **3g**. The cracks of the splats are attributed to the residual stress formation during the

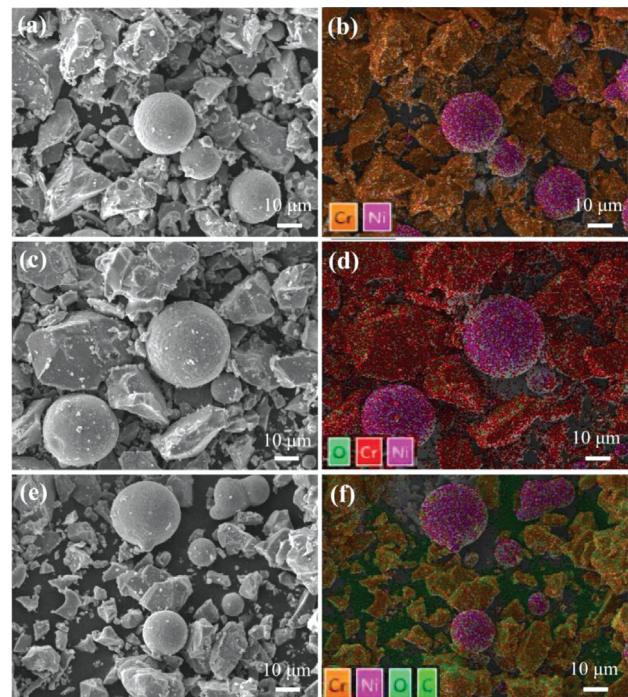


Figure 2: SEM and EDS images of powders: (a–b) Cr₃C₂-NiCr, (c–d) 60 w/% Cr₃C₂-NiCr + 40 w/% NiCr, (e–f) 80 w/% Cr₃C₂-NiCr + 20 w/% NiCr

cooling process after the melted particles hit the substrate. The effect of the melted particles that spread to the surrounding of the hitting point causes the pore formation (Figure 3i).

Based on the EDS measurement, it was found that Cr increased in the coatings consisting of 60 w%

Cr₃C₂-NiCr + 40 w% NiCr and 80 w% Cr₃C₂-NiCr + 20 w% NiCr without sieving (Figures 3d and 3f), contrary to the HVOF coating formed with the original powder (Figure 3b). On the other hand, the Cr element content was reduced in the HVOF coating formed with the powder that was sifted with a 400-mesh sieve (Fig-

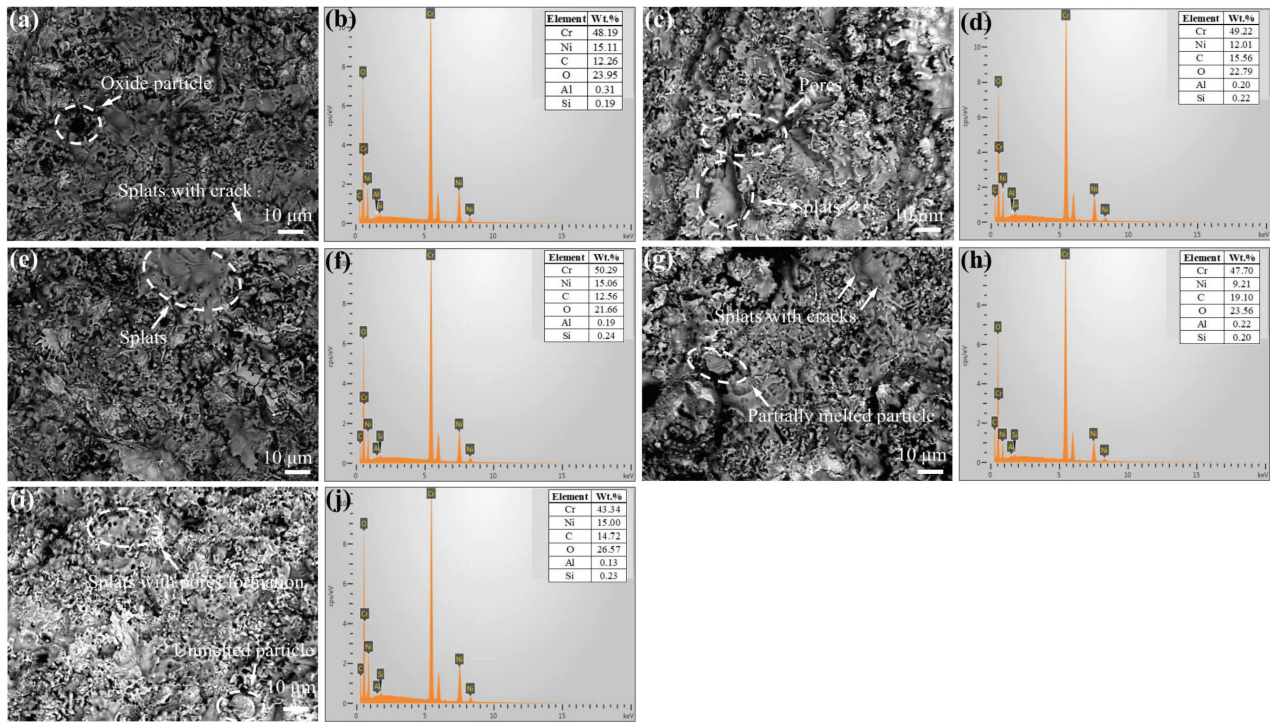


Figure 3: Top-view SEM images and elemental contents of HVOF coatings: (a–b) Cr₃C₂-NiCr, (c–d) 60 w% Cr₃C₂-NiCr + 40 w% NiCr, (e–f) 80 w% Cr₃C₂-NiCr + 20 w% NiCr, and the HVOF coatings composed of the powder that was sifted with a 400-mesh sieve including (g–h) 60 w% Cr₃C₂-NiCr + 40 w% NiCr and (i–j) 80 w% Cr₃C₂-NiCr + 20 w% NiCr

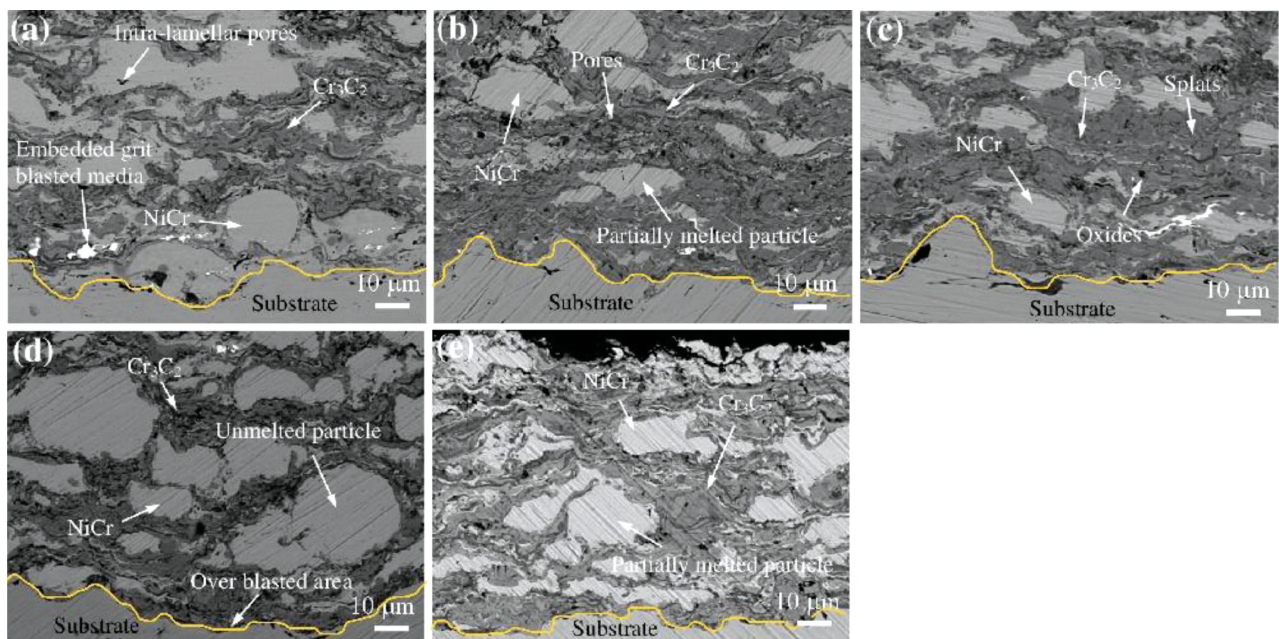


Figure 4: Cross-sectional images of the coatings made by HVOF thermal spray: (a) Cr₃C₂-NiCr, (b) 60 w% Cr₃C₂-NiCr + 40 w% NiCr, (c) 80 w% Cr₃C₂-NiCr + 20 w% NiCr, and the HVOF coatings composed of the powder that was sifted with a 400-mesh sieve including (d) 60 w% Cr₃C₂-NiCr + 40 w% NiCr and (e) 80 w% Cr₃C₂-NiCr + 20 w% NiCr

ures 3h and 3j). In general, the nickel element is reduced, due to the mixing of Cr₃C₂-NiCr with NiCr, in both the coatings with and without sieving with a 400-mesh sieve (Figures 3d, 3f, 3h and 3j). On the other hand, the carbide element was increased due to the mixing of Cr₃C₂-NiCr with NiCr in comparison with the original Cr₃C₂-NiCr powder (Figures 3d, 3f, 3h and 3j).

Cross-sectional images of the following thermal-spray coatings are shown in Figure 4: Cr₃C₂-NiCr (Figure 4a), 60 w/% Cr₃C₂-NiCr + 40 w/% NiCr (Figure 4b), 80 w/% Cr₃C₂-NiCr + 20 w/% NiCr (Figure 4c), the coating obtained with the powder that was sifted with a 400-mesh sieve, i.e., 60 w/% Cr₃C₂-NiCr + 40 w/% NiCr (Figure 4d) and 80 w/% Cr₃C₂-NiCr + 20 w/% NiCr (Figure 4e). Through SEM observations, it was shown that the Cr₃C₂-NiCr coating layers can be successfully deposited onto the substrate (Figures 4a to 4e). Generally, it can be seen that the coating materials can adhere well to the substrate surfaces. The morphology of the layer shows the gradation of dark and light colours, indicating the splats and the unmelted particles, respectively.^{21–23} The light colour of the coating represents the NiCr alloy and the dark colour represents the Cr and C elements. The cross-sectional images show the coating structures, including splats, unmelted particles, partially melted particles, pores, overblasted areas, embedded grit-blasting media and intra-lamellar pores. A splat is a fully melted particle that hits the substrate. To get a good HVOF layer, a splat formation is required. The prerequisites for a splat formation are a flow of powder particles that are small enough and the heat resulting from the HVOF gun flame, able to melt these particles in a very short time. However, when the particle size is high enough but without enough HVOF heat flame energy, particles will remain unmelted or be partially melted.

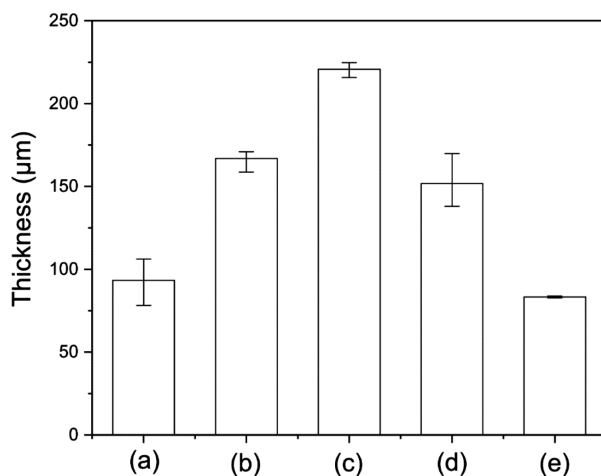


Figure 5: Thickness of the coatings obtained with HVOF thermal spraying: (a) Cr₃C₂-NiCr, (b) 60 w/% Cr₃C₂-NiCr + 40 w/% NiCr, (c) 80 w/% Cr₃C₂-NiCr + 20 w/% NiCr and the HVOF coatings achieved with the powder that was sifted with a 400-mesh sieve including (d) 60 w/% Cr₃C₂-NiCr + 40 w/% NiCr and (e) 80 w/% Cr₃C₂-NiCr + 20 w/% NiCr

Porosity, one of the primary structural flaws in coatings created during thermal spraying, is primarily caused by two factors: shrinkage and gas dynamics in a coating.^{24–26} Due to the substrate (coating) surface roughness, pores are created as a result of gas capture (i.e., at an overblasted area) (Figure 4d) and during the impact, molten droplets deform to create intra-lamellar holes (Figure 4a).^{26,27} The embedded grid-blasted Al₂O₃ in a coating structure indicates the presence of residual particles that were previously used as an abrasive material during the roughing of the substrate surface.

Figure 5 depicts the thickness of the HVOF thermal spray coatings as estimated from the cross-sectional photographs of the deposited coatings. It is demonstrated that the typical coating thickness values of (a) Cr₃C₂-NiCr, (b) 60 w/% Cr₃C₂-NiCr + 40 w/% NiCr, (c) 80 w/% Cr₃C₂-NiCr + 20 w/% NiCr and the HVOF coatings achieved with the powder that was sifted with a 400-mesh sieve including (d) 60 w/% Cr₃C₂-NiCr + 40 w/% NiCr and (e) 80 w/% Cr₃C₂-NiCr + 20 w/% NiCr are ~93.35, 166.9, 220.8, 151.67, 83.3 µm, respectively.

Figure 6 shows the cross-sectional EDS mapping of the HVOF coatings. The elements found in the layer are chromium (Cr), nickel (Ni), carbide (C), oxygen (O), aluminum (Al) and silicon (Si). It is shown that the main coating elements including Cr, Ni, C and O can be seen clearly in the mapping, indicated by different colours including red, pink, green and turquoise, respectively. The mapping shows the general structures of the coatings. The inserted figure at the bottom right corner of each EDS image relates to the Fe element indicated by green (Figures 6a to 6e). The main element of splats is Cr, shown in red (Figures 6a to 6d). Pink indicates the Ni element, whose shape is mainly spherical and irregular (Figures 6a to 6e). Furthermore, these shapes are likely to indicate the unmelted and partially melted particles. The mapping of the O element is very similar to the mapping distribution of the Cr element (Figures 6a to 6e). This indicates that the Cr element forms a compound with the O element to form MnCr₂O₄ as indicated by the XRD spectra at 2θ of around 33.72, 36.29, 42.37° (Figures 7a to 7e) and Cr₂O₃ at 2θ of around 24.56, 33.72, 36.33, 44.19, 97.49° (Figures 7a, 7b, 7d and 7e). These EDS mapping images also reveal that a splat formation is mainly composed of a compound with Cr (Figures 6a to 6e). The presence of Al and Si in the coatings is due to the residual blasting particles (i.e., Al₂O₃, SiO₂) on the surfaces that still stick during the substrate roughing. This is consistent with the cross-sectional SEM images which show that the embedded grit-blasted media, indicated with white, are found in the coatings to have sporadic distributions (Figures 4a to 4e).

Figure 7 shows the XRD spectra of the Cr₃C₂-NiCr coating with a variety of powders including Cr₃C₂-NiCr (Figure 7a), 60 w/% Cr₃C₂-NiCr + 40 w/% NiCr (Figure 7b), 80 w/% Cr₃C₂-NiCr + 20 w/% NiCr (Figure 7c), and the coatings achieved with the powder that was

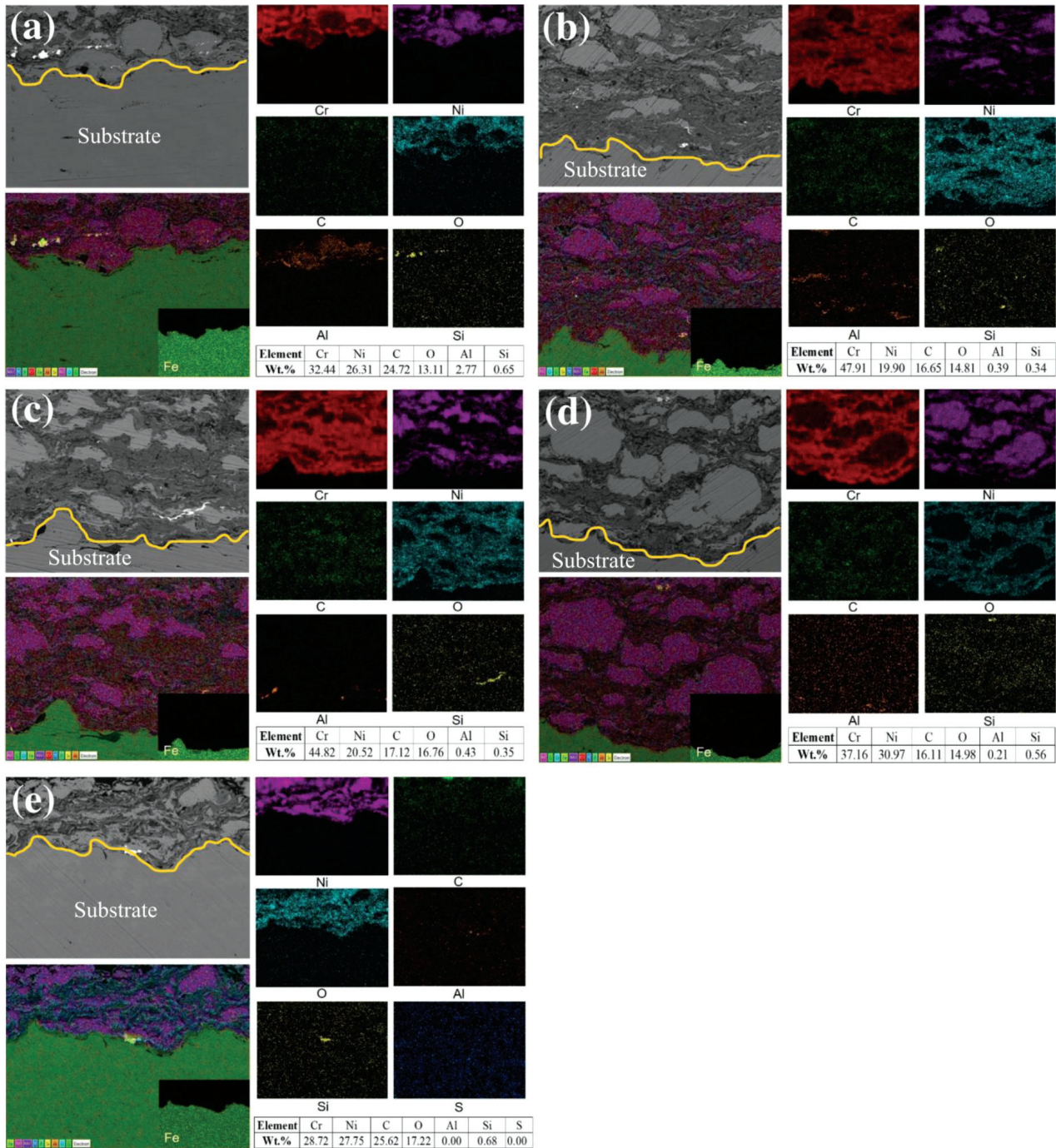


Figure 6: Cross-sectional EDS mapping of the coatings obtained with HVOF thermal spraying: (a) Cr₃C₂-NiCr, (b) 60 w% Cr₃C₂-NiCr + 40 w% NiCr, (c) 80 w% Cr₃C₂-NiCr + 20 w% NiCr and the HVOF coatings achieved with the powder that was sifted with a 400-mesh sieve including (d) 60 w% Cr₃C₂-NiCr + 40 w% NiCr and (e) 80 w% Cr₃C₂-NiCr + 20 w% NiCr

sifted with a 400-mesh sieve including 60 w% Cr₃C₂-NiCr + 40 wt.% NiCr (**Figure 7d**) and 80 w% Cr₃C₂-NiCr + 20 w% NiCr (**Figure 7e**), deposited with HVOF thermal spraying. The major compounds of the coatings are mainly Fe_{0.27}Ni_{0.73}, Cr_{0.22}Ni_{0.78}, Cr₇C₃ and Cr₂O₃ at the 2θ of around 44.17 (**Figures 7a, 7b, 7d and 7e**). It is shown that in comparison to the Cr₃C₂-NiCr coating, the intensity of these phases are generally reduced for 60 w% Cr₃C₂-NiCr + 40 w% NiCr and 80

w% Cr₃C₂-NiCr + 20 w% NiCr coatings (**Figures 7b and 7c**). Conversely, the phases are increased for the coatings obtained with the powder that was sifted with a 400-mesh sieve including 60 w% Cr₃C₂-NiCr + 40 w% NiCr and 80 w% Cr₃C₂-NiCr + 20 w% NiCr (**Figures 7d and 7e**). As the main phases are Cr compounds (i.e., Cr_{0.22}Ni_{0.78}, Cr₇C₃, Cr₂O₃, Cr_{0.1}Fe_{0.9}), the particle size of the powder with Cr₃C₂ is smaller than that of the powder with Ni. This is consistent with the EDS mapping, which

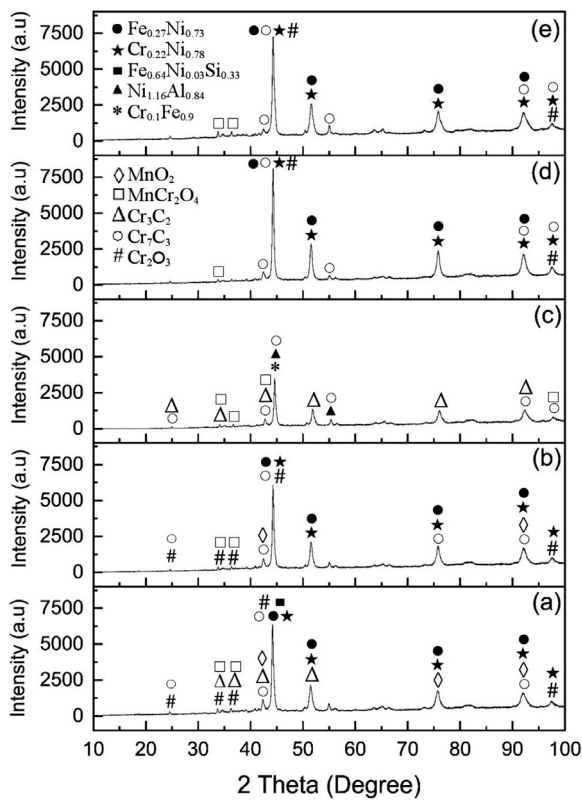


Figure 7: XRD diffraction patterns of the coatings obtained with HVOF thermal spraying: (a) Cr₃C₂-NiCr, (b) 60 w/% Cr₃C₂-NiCr + 40 w/% NiCr, (c) 80 w/% Cr₃C₂-NiCr + 20 w/% NiCr and the HVOF coatings achieved with the powder that was sifted with a 400-mesh sieve including (d) 60 w/% Cr₃C₂-NiCr + 40 w/% NiCr and (e) 80 w/% Cr₃C₂-NiCr + 20 w/% NiCr

shows that the Ni particles are bigger than the Cr particles (**Figures 2b, 2d and 2f**). This condition makes the Cr₃C₂ powder able to pass through the 400-mesh sieve and eventually we can obtain the powder with a Cr₃C₂ content that is larger than that of the powder obtained without sieving. The powder with a larger content of Cr₃C₂ can be used for a HVOF coating with a higher intensity of the phases with a Cr compound (**Figures 7d to 7e**).

We can see the emergence of Mn compounds MnO₂ and MnCr₂O₄ in the HVOF coatings (**Figures 7a to 7e**). As originally manganese existed in the substrate (**Table 1**), this phenomenon indicates that Mn diffuses into the coatings layer. It is similar to some other elements (i.e., Si, C, Fe, Mn) that can move from the substrate to the coating. In the previous research carried out by Premkumar and Balasubramanian, it was found that Si, C and Fe emerge in the scale, which spreads from the substrate to the coating subjected to cyclic oxidation.^{28,29} Furthermore, the study carried out by Sundararajan et al. shows that Mn and Si can also spread from the substrate into the coating due to a high-temperature steam oxidation (i.e., 600–750 °C).^{30,31} XRD spectra revealed the formation of Cr₂O₃ as shown in **Figures 7a, 7b, 7d and 7e**. The following can be used to explain how Cr₂O₃ forms in

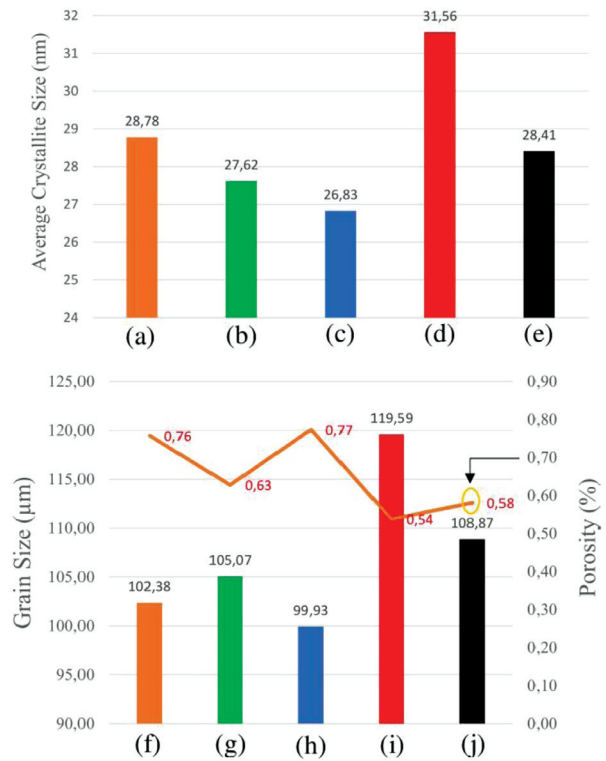


Figure 8: Average crystallite size of the coatings achieved with HVOF thermal spraying: (a) Cr₃C₂-NiCr, (b) 60 w/% Cr₃C₂-NiCr + 40 w/% NiCr, (c) 80 w/% Cr₃C₂-NiCr + 20 w/% NiCr, and the HVOF coating obtained with the powder that was sifted with a 400-mesh sieve including (d) 60 w/% Cr₃C₂-NiCr + 40 w/% NiCr, (e) 80 w/% Cr₃C₂-NiCr + 20 w/% NiCr and the grain size in relation to the level of porosity of (f) Cr₃C₂-NiCr, (g) 60 w/% Cr₃C₂-NiCr + 40 w/% NiCr, (h) 80 w/% Cr₃C₂-NiCr + 20 w/% NiCr, and the HVOF coatings obtained with the powder that was sifted with a 400-mesh sieve including (i) 60 w/% Cr₃C₂-NiCr + 40 w/% NiCr, (j) 80 w/% Cr₃C₂-NiCr + 20 w/% NiCr

NiCr-based coatings: despite the fact that NiO and Cr₂O₃ are stable oxides at a 1 atm oxygen pressure, other factors, particularly kinetics and thermodynamics, may have an impact on the overall scale growth.^{30,32} Compared to nickel, chromium has a stronger affinity for oxygen and produces a more stable oxide.^{30,33} A high temperature during thermal spraying may lead to a reaction of the oxygen in the surroundings with dissociated chromium to form stable Cr₂O₃. According to a report, manganese generally has a negative impact on the oxidation resistance of alloys that create Cr₂O₃.^{30,31} While it does not help the protective film formation, it can diffuse across the Cr₂O₃ film fairly quickly and form a MnCr₂O₄ layer on the surface.^{30,31} It is worth noting that the diffusion of manganese from the substrate into the HVOF Cr₃C₂-NiCr coating and MnCr₂O₄ formation are attributed to the prior emergence of the Cr₂O₃ compound in the HVOF coating.

Figure 8 shows the crystallite and grain sizes as well as the porosity level of the coatings obtained with HVOF thermal spraying. It shows that the crystallite and grain sizes of 60 w/% Cr₃C₂-NiCr + 40 w/% NiCr are bigger

than those of 80 w/% Cr₃C₂-NiCr + 20 w/% NiCr, for both the powders with and without sifting with a 400-mesh sieve (**Figures 8b to 8e** and **8g to 8j**). Generally, the crystallite and grain sizes increase due to the sifting with a 400-mesh sieve as shown for the crystallite sizes of 60 w/% Cr₃C₂-NiCr + 40 w/% NiCr, which are 31.56 nm and 27.62 nm when the coating is obtained from the powders with and without a sifting process, respectively (**Figures 8b** and **8d**). This trend is consistent with the crystallite sizes of the 80 w/% Cr₃C₂-NiCr + 20 w/% NiCr coatings, which are 28.41 nm and 26.83 nm for the coatings obtained with the powder with and without sifting with a 400-mesh sieve, respectively (**Figures 8c** and **8e**).

These phenomena show that the grain sizes are increased due to the sifting with a 400-mesh sieve of both 60 w/% Cr₃C₂-NiCr + 40 w/% NiCr and 80 w/% Cr₃C₂-NiCr + 20 w/% NiCr coatings (**Figures 8g to 8j**). The sifting with a 400-mesh sieve enables us to obtain a powder with a size of 400 mesh and lower. During the deposition with HVOF thermal spraying, a powder with a low size can absorb the heat of the HVOF gun flame better than a powder with a bigger size. A powder with a small size has a larger surface area than a powder with a bigger size. As a result, a larger number of particles from the sifted powder can be melted enough to form a fully melted droplet, which eventually leads to crystallites and grains with bigger dimensions. The grain sizes of all coatings are bigger than crystallite sizes as a grain can be either a single crystalline or polycrystalline structure as shown in **Figure 8**.

One of the important characteristics of a coating, obtained with thermal spraying is porosity. Although pores are unavoidable in the coatings, obtained with thermal spraying, they can be minimized through a proper deposition. Normally the porosity level of an HVOF coating is around 0.1 % to 2 %.³⁴ It was shown that the porosity of the Cr₃C₂-NiCr, 60 w/% Cr₃C₂-NiCr + 40 w/% NiCr, 80 w/% Cr₃C₂-NiCr + 20 w/% NiCr coatings and the HVOF coatings achieved with the powder that was sifted with a 400-mesh sieve including 60 w/% Cr₃C₂-NiCr + 40 w/% NiCr and 80 w/% Cr₃C₂-NiCr + 20 w/% NiCr are (0.76, 0.63, 0.77, 0.54, 0.58) %, respectively (**Figures 8f to 8j**). These values indicate a successful deposition as the pore formations in all deposited coatings are relatively low, in a range of 0.54–0.77 %. This clearly shows that the powder size obtained with the 400-mesh sieve can reduce the porosity level of the coating (**Figures 8i to 8j**). A powder with a small grain size leads to the production a large quantity of fully melted droplets, which eventually results in an HVOF-deposited layer with a higher density of formed splats. The intensified contact among the splats can reduce the pores and oxide formations.^{35,36} As a result, the pore formation can be minimized. It can be deduced that decreasing the powder size with a sifting process improves the quality of HVOF

coatings. In relation to the grain size, it can be seen that the porosity level decreased by increasing the grain size.

4 CONCLUSIONS

A successful deposition of Cr₃C₂-NiCr layers onto a medium-carbon steel substrate was achieved using HVOF thermal spraying, as demonstrated by substrate surfaces that can hold coating elements firmly, exhibiting a porosity of up to 0.77 %. When compared to 80 w/% Cr₃C₂-NiCr + 20 w/% NiCr, it was found that the crystallite and grain sizes of 60 w/% Cr₃C₂-NiCr are larger. Furthermore, the crystallite and grain sizes can be increased through a sifting process using a 400-mesh sieve. As smaller-sized powders have more surface area, more particles from a sifted powder can combine to create totally melted droplets, ultimately leading to crystallites and grains with larger dimensions. In terms of pore development, better melted droplets allow for the production of an HVOF layer with a higher density. Voids and oxide deposits can be lessened by an enhanced splat contact. It is obvious that the powder sifted with a 400-mesh filter, i.e., 60 w/% Cr₃C₂-NiCr + 40 w/% NiCr, has the best powder composition as it achieves the lowest porosity of 0.54 %. The oxidation resistance of the alloys that form Cr₂O₃ is typically adversely affected by manganese. This element does not promote the formation of a preservative coating, but it has a tendency to disperse over the Cr₂O₃ film fairly quickly to form a MnCr₂O₄ layer on the surface. It should be noted that the emergence of the Cr₂O₃ compound in the HVOF layer causes the diffusion of manganese from the substrate into the Cr₃C₂-NiCr layer and the establishment of MnCr₂O₄.

Acknowledgment

The authors thank Advanced Characterization Laboratories Bandung, National Research and Innovation Agency E-Layanan Sains for providing the facilities and scientific and technical support. This work was supported by Rumah Program Nanoteknologi dan Material Maju Tahun 2023 - ORNM BRIN, National Research and Innovation Agency of the Republic of Indonesia (Grant No. 3/III.10/HK/2023).

Declarations

Jason Lauzuardy and Edy Riyanto are the main contributors. The authors declare that they have no competing interests.

5 REFERENCES

- ¹ V. Matikainen, S. R. Peregrina, N. Ojala, H. Koivuluoto, J. Schubert, Š. Houdková, P. Vuoristo, Erosion wear performance of WC-10Co4Cr and Cr₃C₂-25NiCr coatings sprayed with high-velocity thermal spray processes, *Surf. Coat. Technol.*, 370 (2019), 196–212, doi:10.1016/j.surfcoat.2019.04.067

- ² S. Hong, Y. Wu, W. Gao, J. Zhang, Y. Zheng, Y. Zheng, Slurry erosion-corrosion resistance and microbial corrosion electrochemical characteristics of HVOF sprayed WC-10Co-4Cr coating for offshore hydraulic machinery, *Int. J. Refract. Met. Hard Mater.*, 74 (2018), 7–13, doi:10.1016/j.ijrmhm.2018.02.019
- ³ S. Septianissa, B. Prawara, E. A. Basuki, E. Martides, E. Riyanto, Improving the hot corrosion resistance of γ/γ' in Fe-Ni superalloy coated with Cr₃C₂-20NiCr and NiCrAlY using HVOF thermal spray coating, *Int. J. Electrochem. Sci.*, 17 (2022), 221231, doi:10.20964/2022.12.27
- ⁴ J. A. Picas, S. Menargues, E. Martin, M. T. Baile, Cobalt free metallic binders for HVOF thermal sprayed wear resistant coatings, *Surf. Coat. Technol.*, 456 (2023), 129243, doi:10.1016/j.surfcoat.2023.129243
- ⁵ S. Singh, K. Goyal, R. Bhatia, A review on protection of boiler tube steels with thermal spray coatings from hot corrosion, *Mater. Today: Proc.*, 56 (2022), 379–383, doi:10.1016/j.matpr.2022.01.219
- ⁶ N. Vashishtha, S. G. Sapate, Abrasive wear maps for high velocity oxy fuel (HVOF) sprayed WC-12Co and Cr₃C₂-25NiCr coatings, *Tribol. Int.*, 114 (2017), 290–305, doi:10.1016/j.triboint.2017.04.037
- ⁷ V. Matikainen, H. Koivuluoto, P. Vuoristo, A study of Cr₃C₂-based HVOF- and HVAF-sprayed coatings: Abrasion, dry particle erosion and cavitation erosion resistance, *Wear*, 446–447 (2020), 203188, doi:10.1016/j.wear.2020.203188
- ⁸ L. M. Berger, Application of hardmetals as thermal spray coatings, *Int. J. Refract. Metals Hard Mater.*, 49 (2015), 350–364, doi:10.1016/j.ijrmhm.2014.09.029
- ⁹ X. Zhang, F. Li, Y. Li, Q. Lu, Z. Li, Haiyang Lu, Xueju Ran, Xiaoxia Qi, Comparison on multi-angle erosion behavior and mechanism of Cr₃C₂-NiCr coatings sprayed by SPS and HVOF, *Surf. Coat. Technol.*, 403 (2020), 126366, doi:10.1016/j.surfcoat.2020.126366
- ¹⁰ V. Matikainen, G. Bolelli, H. Koivuluoto, P. Sassatelli, L. Lusvardi, P. Vuoristo, Sliding wear behavior of HVOF and HVAF sprayed Cr₃C₂-based coatings, *Wear*, 388–389 (2017), 57–71, doi:10.1016/j.wear.2017.04.001
- ¹¹ J. A. Picas, M. Punset, E. Rupérez, S. Menargues, E. Martin, M. T. Baile, Corrosion mechanism of HVOF thermal sprayed WC-CoCr coatings in acidic chloride media, *Surf. Coat. Technol.*, 371 (2019), 378–388, doi:10.1016/j.surfcoat.2018.10.025
- ¹² G. Bolelli, V. Cannillo, L. Lusvardi, S. Ricco, Mechanical and tribological properties of electrolytic hard chrome and HVOF-sprayed coatings, *Surf. Coat. Technol.*, 200 (2006), 2995–3009, doi:10.1016/j.surfcoat.2005.04.057
- ¹³ J. R. Davis, *Handbook of thermal spray technology*, ASM International, Materials Park, Ohio 2004, 47–56
- ¹⁴ B. Pratap, V. Bhatt, V. Chaudhary, A Review on thermal spray coating, *Int. J. Eng. Res.*, 10 (2015), 25474–25481
- ¹⁵ N. F. Ak, C. Tekmen, I. Ozdemir, H. S. Soykan, E. Celik, NiCr coatings on stainless steel by HVOF technique, *J. Surf. Coat. Technol.*, 174–175 (2003), 1070–1073, doi:10.1016/S0257-8972(03)00367-0
- ¹⁶ N. Abu-Warda, G. Boissonnet, A. J. López, F. Pedraza, Analysis of thermo-physical properties of NiCr HVOF coatings on T24, T92, VM12 and AISI 304 steels, *Surf. Coat. Technol.*, 416 (2021), 127163, doi:10.1016/j.surfcoat.2021.127163
- ¹⁷ J. A. Picas, A. Forn, R. Rilla, E. Martin, HVOF thermal sprayed coatings on aluminium alloy and aluminium matrix composites, *J. Surf. Coat. Technol.*, 200 (2005), 1178–1181, doi:10.1016/j.surfcoat.2005.02.124
- ¹⁸ S. Matthews, M. Bhagvandas, L.-M. Berger, Creation of modified Cr₃C₂-NiCr hardmetal coating microstructures through novel processing, *J. Alloys Compd.*, 824 (2020), 153868, doi:10.1016/j.jallcom.2020.153868
- ¹⁹ ASME SA-210/SA-210M, Standard Specification for seamless medium-carbon steel boiler and superheater tubes, The American Society of Mechanical Engineering, New York 2019, 279–284
- ²⁰ M. Oksa, J. Metsajoki, Optimizing NiCr and FeCr HVOF coating structures for high temperature corrosion protection applications, *J. Therm. Spray Technol.*, 24 (2015), 436–453, doi:10.1007/s11666-014-0192-0
- ²¹ J. He, M. Ice, E. Lavernia, Particle melting behaviour during high-velocity oxygen fuel thermal spraying, *J. Therm. Spray Technol.*, 10 (2001), 83–93, doi:10.1361/105996301770349547
- ²² V. V. Sobolev, J. M. Guilemany, A. J. Martin, Flattening of Composite Powder Particles during Thermal Spraying, *J. Therm. Spray Technol.*, 6 (1997), 353–360, doi:10.1007/s11666-997-0070-0
- ²³ R. S. Neiser, M. F. Smith, R. C. Dykhuizen, Oxidation in wire HVOF sprayed steel, *J. Therm. Spray Technol.*, 7 (1998), 537–545, doi:10.1361/105996398770350765
- ²⁴ G. C. Ji, C. J. Li, Y. Y. Wang, W. Y. Li, Erosion Performance of HVOF-Sprayed Cr₃C₂-NiCr Coatings, *J. Therm. Spray Technol.*, 16 (2007), 557–565, doi:10.1007/s11666-007-9052-5
- ²⁵ W. D. Callister, *Material Science and Engineering: An Introduction*, John Wiley and Sons, Inc., New York 2007
- ²⁶ V. V. Sobolev, J. M. Guilemany, Analysis of coating gas porosity development during thermal spraying, *Surf. Coat. Technol.*, 70 (1994), 57–68, doi:10.1016/0257-8972(94)90075-2
- ²⁷ V. V. Sobolev, J. M. Guilemany, Investigation of coating porosity formation during high velocity oxy-fuel (HVOF) spraying, *Mater. Lett.*, 18 (1994), 304–308, doi:10.1016/0167-577X(94)90012-4
- ²⁸ K. Premkumar, K. R. Balasubramanian, Evaluation of cyclic oxidation behavior and mechanical properties of nanocrystalline composite HVOF coatings on SA 210 grade C material, *J. Eng. Fail. Anal.*, 97 (2019), 635–644, doi:10.1016/j.engfailanal.2019.01.038
- ²⁹ J. Robertson, M. I. Manning, Healing layer formation in Fe–Cr–Si ferritic steels, *Mater. Sci. Technol.*, 5 (1989), 741–753, doi:10.1179/mst.1989.5.8.741
- ³⁰ T. Sundararajan, S. Kuroda, K. Nishida, T. Itagaki, F. Abe, Behaviour of Mn and Si in the spray powders during steam oxidation of Ni–Cr thermal spray coatings, *ISIJ Int.*, 44 (2004), 139–144, doi:10.2355/ISIJINTERNATIONAL.44.139
- ³¹ F. H. Stott, F. I. Wei, C. A. Enahoro, The influence of manganese on the high-temperature oxidation of iron-chromium alloys, *Corros. Mater.*, 40 (1989), 198–205, doi:10.1002/maco.19890400403
- ³² S. Kumar, M. Kumar, A. Handa, Comparative study of high temperature oxidation behavior and mechanical properties of wire arc sprayed Ni-Cr and Ni-Al coatings, *Eng. Fail. Anal.*, 106 (2019), 104173, doi:10.1016/j.engfailanal.2019.104173
- ³³ F. H. Stott, G. C. Wood, Internal oxidation, *Mater. Sci. Technol.*, 4 (1988) 12, 1072, doi:10.1179/mst.1988.4.12.1072
- ³⁴ B. Bhushan, B. K. Gupta, *Handbook of Tribology: Materials, Coatings, and Surface Treatments*, McGraw-Hill, New York 1991
- ³⁵ G. B. Sucharski, A. G. M. Pukaszewicz, R. F. Vaz, R. S. C. Paredes, Optimization of the deposition parameters of HVOF FeMnCrSi+Ni+B thermally sprayed coatings, *Soldag. Insp.*, 20 (2015), 238–252, doi:10.1590/0104-9224/SI2002.11
- ³⁶ V. V. Sobolev, J. M. Guilemany, Effect of oxidation on droplet flattening and splat-substrate interaction in thermal spraying, *J. Therm. Spray Technol.*, 8 (1999), 523–530, doi:10.1361/105996399770350205